

Cell-free Protein Synthesis in a Microchamber Revealed the Presence of an Optimum Compartment Volume for High-order Reactions

Taiji Okano,[†] Tomoaki Matsuura,^{†,‡} Hiroaki Suzuki,^{†,§} and Tetsuya Yomo^{*,†,||,⊥}

[†]Exploratory Research for Advanced Technology, Japan Science and Technology Agency, 1-5 Yamadaoka, Suita, Osaka 565-0871, Japan

[‡]Department of Biotechnology, Graduate School of Engineering, Osaka University, 2-1 Yamadaoka, Suita, Osaka 565-0871, Japan

[§]Department of Precision Mechanics, Chuo University, 1-13-27 Kasuga, Bunkyo-ku, Tokyo 112-8551, Japan

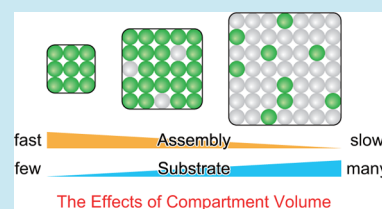
^{||}Department of Bioinformatic Engineering, Graduate School of Information Science and Technology, Osaka University, 1-5 Yamadaoka, Suita, Osaka 565-0871, Japan

[⊥]Graduate School of Frontier Biosciences, Osaka University, 1-5 Yamadaoka, Suita, Osaka 565-0871, Japan

Supporting Information

ABSTRACT: The application of microelectromechanical systems (MEMS) to chemistry and biochemistry allows various reactions to be performed in microscale compartments. Here, we aimed to use the glass microchamber to study the compartment size dependency of the protein synthesis, one of the most important reactions in the cell. By encapsulating the cell-free protein synthesis system with different reaction orders in femtoliter microchambers, chamber size dependency of the reaction initiated with a constant copy number of DNA was investigated. We were able to observe the properties specific to the high order reactions in microcompartments with high precision and found the presence of an optimum compartment volume for a high-order reaction using real biological molecules.

KEYWORDS: microchamber, compartmentalization, *in vitro* transcription and translation, PURE system, protein synthesis



Microcompartmentalization has become one of the standard techniques for biochemical studies.^{1–6} The measurement of various reactions, including enzymatic reactions, ligand binding, and protein synthesis, in volumes ranging from 1 nL to 1 fL, has been shown with the use of microchambers and emulsion microdroplets. The common advantages in using microcompartmentalization are 2-fold: the high-throughput (parallel) experiments and single-cell/molecule resolution are feasible.^{7–13} The size of these microcompartments can be easily controlled and adjusted;^{14,15} therefore, in addition to the advantages mentioned above, microcompartments can be used to study the compartment size dependency of the chemical and biochemical reactions.^{16,17}

Living cells exhibit dynamic properties with respect to their compartments. The size and shape of a compartment can change depending on the cell cycle and in response to the external environment.^{18–21} In contrast with such a dynamic property, the cell also shows a static property, that is, it maintains the copy number of the genome constant. How is the static property influenced by the dynamic property of the compartment size? For example, protein synthesis decodes the genome, which is present in a constant copy number within the cell, while the size of the compartment changes. How is such protein synthesis affected by the compartment size? In particular, the protein synthesis involves an assembly of multiple molecules that could be high-order reactions, whose rate is highly sensitive to concentration changes.^{22,23} In this paper, we thus ask how the protein synthesis triggered by a

constant copy number of DNA but with different reaction orders is influenced by the compartment size.

We have recently performed protein synthesis with a different reaction order within emulsion droplets whose average volumes range from femtoliter to microliter using a cell-free protein synthesis system, and observed the acceleration of only the high-order reaction through compartmentalization.²⁴ However, because the droplet volume in the same batch was distributed by over 2 orders of magnitude, the effects of compartment volume on the protein synthesis with a constant copy number of DNA were not measurable. To overcome this problem, we recently fabricated solid glass microchambers with cell-sized volumes and demonstrated that the protein synthesis from a single DNA copy can be detected with high precision.²⁵ Consequently, precise control over the compartment volume has now become possible, and its effects on the protein synthesis can be examined.

In this study, we performed protein synthesis with different reaction orders in microcompartments with three different volumes but with a constant copy number of DNA molecules to investigate the effects of compartment volume on the reaction kinetics. We used glass microchambers and enclosed a reconstituted *in vitro* transcription/translation system (IVTT),

Special Issue: Cell-Free Synthetic Biology

Received: July 23, 2013

Published: August 30, 2013

the PURE system,^{26–28} together with DNA encoding the reporter protein β -glucuronidase (GUS) or β -galactosidase (GAL). GUS and GAL synthesis were found to be a fourth- and a first-order reaction, respectively.²⁹ The GUS and GAL are enzymes that assemble into tetramers^{30,31} starting with monomer to dimer assembly, followed by dimer to tetramer (Figure 1a). Tetramers are the only form that exhibits catalytic

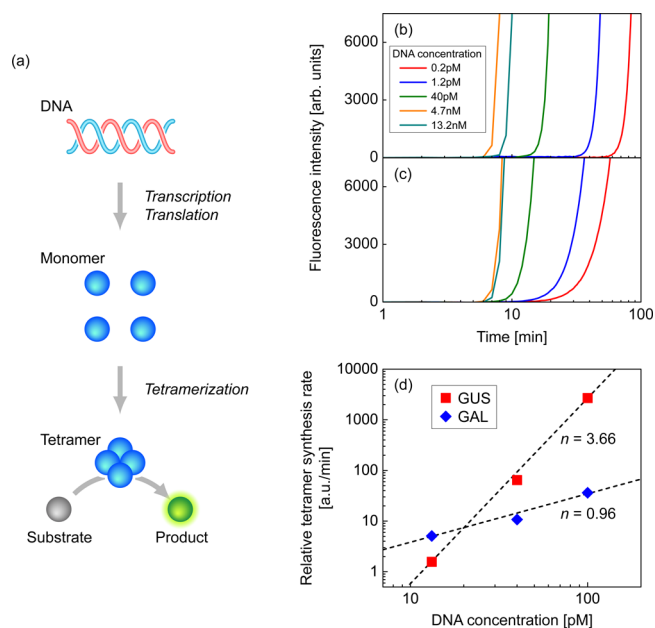


Figure 1. (a) Schematic diagram of the GUS and GAL syntheses. The DNA encoding the GUS and GAL was added to the reconstituted *in vitro* translation/transcription system (IVTT), the PURE system. The presence of a fluorogenic substrate, TG-GlcU or TG- β Gal, both of which emit green fluorescence only after hydrolysis, allowed the detection of the tetrameric GUS and GAL, respectively. (b, c) Time courses for the (b) GUS and (c) GAL syntheses in bulk. The difference between GUS and GAL synthesis is the rate-limiting step of the reaction.²⁴ The rate of GUS synthesis is limited by the monomer-to-tetramer assembly, whereas that of GAL synthesis is limited by the monomer synthesis step. Thus, theoretically, the GUS and GAL syntheses are approximated as fourth- and first-order reactions, respectively. Both reactions exhibited a concave curve. (d) Estimation of the reaction order for the GUS and GAL syntheses in bulk. Relative tetramer synthesis rates ($d[T]/dt$) for GUS and GAL were determined using the second derivative of the time course data at 11 and 5 min, respectively. The dotted lines indicate the fit with $\log(d[T]/dt) = \log A + n \log[DNA]$, in which A is a constant and n is the reaction order. The composition of the reaction mixture was the same as in the microchamber experiments.

activity. In the IVTT system used, the rate of monomeric protein synthesis obeyed the Michaelis–Menten kinetics: it was linearly related to the DNA concentration,²⁹ that is, $d[\text{monomer}]/dt \propto [DNA]$, at a DNA concentration below saturation. With the reaction shown in Figure 1a, however, the reaction order can be different depending on the values of the rate constants, which we describe below.

We first confirmed the reaction order of the GUS and GAL syntheses provided in our previous report.²⁹ The GUS and GAL syntheses were performed in the presence of their fluorogenic substrates (TG-GlcU and TG- β Gal, respectively).³² The synthesis of two enzymes could be detected in real time by the increase in the fluorescence signal from TG, the fluorescent product. Parts b and c of Figure 1 provide the time course data

of the bulk GUS and GAL syntheses, respectively. Both reactions presented a concave curve, which was interpreted as the result of a multistep reaction (e.g., transcription, translation, assembly, and substrate hydrolysis).²⁴ Based on the time course data, relationship between relative tetramer synthesis rate ($d[T]/dt$) and the DNA concentration ($[DNA]$) was plotted to obtain n , the reaction order (Figure 1d). Relative tetramer synthesis rate was estimated from the second derivative of the fluorescence intensity FI (d^2FI/dt^2). $d[T]/dt$ and $[DNA]$ were in high-order ($n = 3.66$) and linear ($n = 0.96$) relationships with GUS and GAL, respectively. Consistent with our previous study,²⁹ these data indicate that GUS and GAL reaction can be approximated as fourth- and first-order reactions ($FI \propto [DNA_{GUS}]^4$ and $FI \propto [DNA_{GAL}]^1$), respectively. The difference between GUS and GAL can be described by the difference in the rate-limiting step of the reaction. The rate-limiting step is identified as the monomer-to-tetramer assembly for GUS. In contrast, for GAL synthesis, the tetramerization is rapid and the monomer synthesis is the rate-limiting step.²⁹

We conducted the GUS and GAL synthesis, starting from the constant copy number of DNA, in the glass microchambers of three different volumes (56, 126, and 350 fL) to investigate the size dependency of these reactions (see Methods). The dimensions of the chambers were $4 \times 4 \times 3.5 \mu\text{m}$, $6 \times 6 \times 3.5 \mu\text{m}$, and $10 \times 10 \times 3.5 \mu\text{m}$. We enclosed 70 DNA molecules that encode GUS (GAL) within the chambers of different volumes together with the IVTT reaction mixture and monitored the fluorescent product TG (Figure 2a,b). The concentrations of all components except the DNA, such as the IVTT components, were constant irrespective of the chamber volume. A large variation in the time course for GUS synthesis was observed among the different chamber volumes. The lag time τ , defined as the time required to reach the threshold number of TG (10^6 molecules), was smaller in the smaller chambers (Figure S1a, Supporting Information), which indicates that the tetrameric GUS synthesis was accelerated in a smaller chamber. In contrast, for GAL, the production of TG began increase with a similar time course in chambers with different volumes (Figure 2b). The difference between the GUS and GAL can be interpreted as the difference in the reaction order. The high-order reaction is compartment-volume dependent, but the first-order reaction is independent (see equations in the Supporting Information). Alternatively, the difference can be described by the difference in the rate-limiting step. In the GUS synthesis, the rate-limiting step is the monomer-to-tetramer assembly, and the assembly from a constant number of monomers is compartment-volume dependent. In the GAL synthesis, the rate-limiting step is the monomer synthesis, which is not a volume-dependent reaction. The GUS and GAL syntheses exhibited properties that are consistent with their high- and first-order reaction kinetics, respectively.

The precision and reproducibility of the GUS and GAL syntheses in the glass microchamber were high, with a coefficient of variation (CV) of 10% in a plateau region using the data from 50 different chambers. Because the tetrameric GUS and GAL syntheses are high-order reactions with respect to time, the CV maximum value was 80% in the region in which TG increased over time. Nevertheless, the effects of the chamber volume on the GUS and GAL syntheses could be quantitatively assessed using average values. The lag time τ for both reactions at different chamber volumes was in agreement with the theoretical prediction (Figure S1a, Supporting

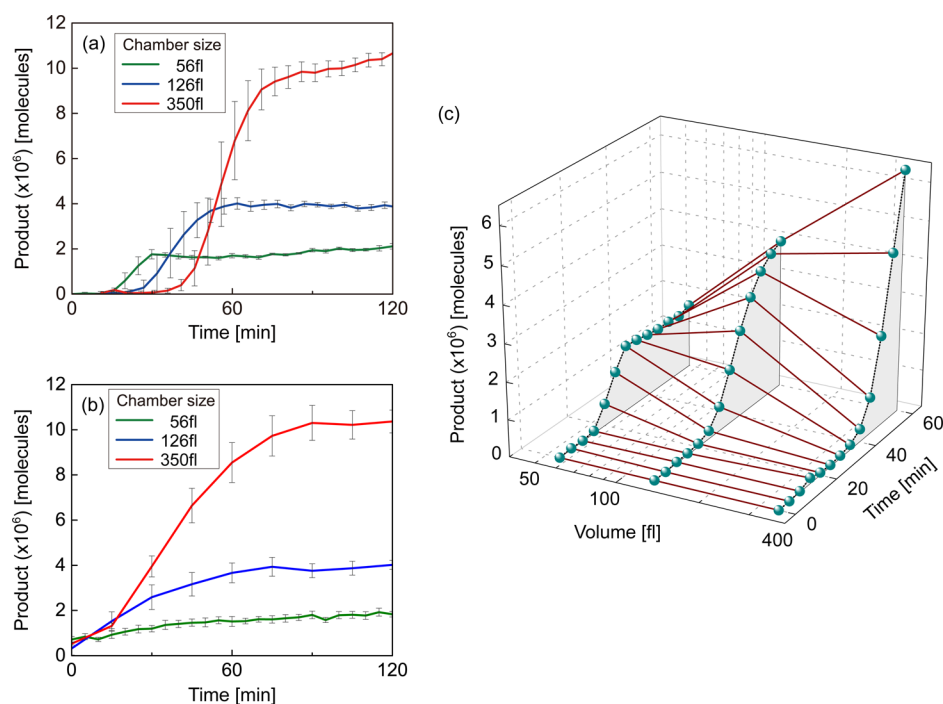


Figure 2. Time courses for the GUS and GAL syntheses in microchambers. (a) The GUS synthesis from 70 copies of DNA in chambers of three different volumes (56 fL, 126 fL, and 350 fL). The DNA concentrations were 2.1 nM (56 fL), 923 pM (126 fL), and 332 pM (350 fL). A large variation in the time course was observed among the chamber volumes. (b) The GAL synthesis under the same conditions as GUS. The fluorescent product TG began to increase with similar timing, irrespective of the chamber volume. (c) A three-dimensional plot of the GUS synthesis. At an earlier time (<30 min), a negative correlation was observed between the TG yield and the chamber volume as the TG began to increase in a smaller chamber. A positive correlation between the TG yield and the chamber volume was observed after adequate time had elapsed (>50 min). A competition between these properties led to an inverted U-shaped correlation in the intermediate times (35–45 min). The results represent data averaged over 50 different chambers. The data were acquired at 5 min intervals (15 min intervals in some experiments). The error bars represent the standard deviation among 50 chambers.

Information). For GUS and GAL, the production of TG reached a plateau after sufficient time had elapsed likely due to the complete hydrolysis of the fluorogenic substrate. In fact, the product yield estimated from the fluorescence intensity was highly correlated with that determined from the substrate concentration (Figure S1b, Supporting Information). Using the microchamber, we succeeded in conducting the reactions in parallel and obtaining data with high precision. Green fluorescent protein (GFP) synthesis using the IVTT was reported to proceed faster in smaller compartments,¹⁷ which is similar to what we observed with the GUS synthesis. While the mechanism of the acceleration with the GFP synthesis remains unclear, measurements with high precision in the current study contributed in clarifying the mechanism of acceleration of the GUS synthesis.

When the reaction was triggered by a constant number of information molecules, or DNA, the fluorescent product (TG) begins to increase earlier in the smaller chamber for the GUS synthesis due to faster tetramerization (Figure 2a). However, the TG increase stops earlier in the smaller chamber due to the more rapid complete hydrolysis of the substrate in the smaller chamber (Figure 2a, plateau). Under such circumstances, an optimum compartment volume must exist in which the TG quantity is maximized. To clarify this point, the number of TG molecules obtained in each chamber was plotted in three dimensions (Figure 2c). More TG was produced in a smaller chamber during the first 35 min. Between 40 and 50 min, the reaction in the 56-fL chamber terminated due to the complete hydrolysis of the fluorogenic substrate, while the reaction

continued in the larger volume. During this time, the TG yield was maximized in 126 fL. The maximum compartment volume is the result of two constraints: With a high-order reaction triggered from a fixed number of information molecules, the smaller compartment contains more products earlier because a high-order reaction proceeds faster in a smaller compartment. However, over time, the smaller compartment contains fewer products because smaller compartments have fewer substrates. In the interim, a compartment volume can be found in which the quantity of product is maximized.

Cell volumes vary over a wide range, from 1 fL to 1 μ L, depending on the species and/or organ, but cells of the same type remain within a certain size range.^{33,34} To explain the mechanism by which the cell size is maintained, the existence of an optimum cell size for cellular functions has been studied. For example, if cells are too small, the biomolecules are condensed and diffusion is slow. Conversely, if cells are too large, the time required for the molecules to diffuse across the entire cell increases. An intermediate (optimum) size exists in which the time required for the macromolecules to diffuse throughout the cell is minimized.³⁵ In addition to the idea of an optimum size, other concepts have been proposed as the mechanism by which the cell size is maintained.^{34,36}

Our results offer one explanation for the mechanism by which the cell size is maintained. Many macromolecular complexes exist in a cellular compartment, and many of these complexes exhibit their functions only after assembly.³⁷ The assembly processes of these complexes could be high-order reactions, which are affected by the compartment volume. Like

the GUS synthesis, a high-order reaction has the potential for an optimum size in which the product quantity is maximized. If the number of product molecules correlates with the fitness of the cell, an optimum cell size will be selected through an evolutionary process. For example, if one assumes that the assembly of genomic DNA and DNA polymerase, whose numbers are held constant, is a high-order reaction, the polymerase and genomic DNA complex will be more abundant in smaller compartments after a shorter interval. However, small compartments have fewer substrates. When the deoxynucleotides—the substrates of the polymerase reaction—exist in a compartment at the same concentration irrespective of the compartment volume, the substrate is depleted in a small compartment before the genome replication is complete. In such situations, an optimum compartment volume can be found in which the genome replication is completed first. The genome replication rate correlates with the fitness of the cells, and an optimum cell size in which the genome replication rate is maximized will be selected through an evolutionary process.

To investigate the effects of the compartment volume on a high-order reaction, we performed syntheses of the tetrameric GUS and GAL in cell-sized glass-microchambers using IVTT, which was triggered by a constant copy number of DNA. We succeeded in conducting the parallel reactions and obtaining data with high precision (CV = 10%). Furthermore, we found that because the GUS synthesis is a high-order reaction, it has an optimum compartment volume in which the quantity of fluorescent product is maximized. In living cells, many gene products that are involved in cellular reactions are produced from a single set of genomic DNA within a compartment. While our artificial system differs significantly from living cells, it can be considered a simple cellular model. Because living cells dynamically change their size and shape, studying the effects of compartment volume through *in vivo* experiments can prove difficult. In contrast, our system enables the free design of a cell model to demonstrate existence of an optimum volume for maximizing the reaction products using real biological molecules. By constructing increasingly complex systems, a study of the fundamental rules and principles underlying living organisms becomes possible.^{38–42}

METHODS

***In Vitro* Transcription and Translation Systems.** The plasmids encoding the GUS and GAL, pET-gusA and pET-lacZ, respectively, were constructed as previously described.⁴³ The templates used for the *in vitro* transcription/translation (IVTT) were prepared via PCR amplification of the corresponding plasmid using the T7F (5'-TAATACGACTCACTATAGGG-3') and T7R (5'-GCTAGTTATTGCTCAGCGG-3') primers with PYRObest DNA polymerase (Takara) according to the manufacturer's instructions and purified using a QIAquick PCR purification kit (Qiagen). The DNA concentrations were determined from the absorbance at 260 nm. A reconstituted IVTT (PURE²⁶) system was used in this study that was modified according to previous studies.^{27,28} The composition was as previously described.⁴³ For the GUS and GAL syntheses, template DNA (the PCR product) was added to the IVTT and was supplemented with 4 units of RNasin (Promega), 100 nM Alexa Fluor 594 (Invitrogen) as an internal reference dye, and 50 μ M fluorogenic substrate TokyoGreen-GlcU (TG-GlcU) or TokyoGreen- β Gal (TG- β Gal) (Sekisui Medical). The TG-GlcU and TG- β Gal do not

fluoresce prior to hydrolysis, but yield TG, a fluorescent product that emits green fluorescence as a result of hydrolysis.

Microchamber Fabrication. We fabricated microchambers of glass (quartz) to monitor the protein synthesis using the IVTT. As we reported,²⁵ a chamber array structure was fabricated on a quartz substrate via reactive ion etching. Then, we fabricated a thin poly(dimethylsiloxane) (PDMS) layer (400 nm) on top of the chamber as an adhesion layer for the glass substrate that served as a lid.⁴⁴ To form the closed compartments, the open side of the glass microchamber was sealed with a coverslip after introducing the reagent. A silicone-coated coverslip (C2210; Matsunami) blocked with 1% bovine serum albumin (BSA) was used due to its good adhesion to the PDMS layer on the microchambers. The microchamber and the coverslip were blocked with 0.88 mM amino acids (20 amino acids dissolved in water) to reduce any surface effects on the reaction. The blocking procedure was performed by immersing the chamber and the coverslip in the amino acid reagent overnight at room temperature. After the microchamber was washed with pure water, the reaction solution was placed in the microchamber and covered with the coverslip. Any excess solution was forced out by clamping the microchamber in a vice.

Observations. Real-time measurements were carried out in the test tube (bulk measurements) using a real-time PCR system (Mx3005P; Agilent). The filter sets used for measuring the fluorescence intensities of the TG and Alexa Fluor 594 were 492/516 and 635/665 nm (excitation/emission wavelengths), respectively.

The microchambers used in this study were observed using a fluorescence microscope (TE2000; Nikon) equipped with a 20 \times /NA0.75 objective, a CCD camera (DV887; Andor Technology), and a filter set (excitation 472.5 nm, emission 520 nm). Microscopic images were acquired at 5 min intervals (15 min intervals in some experiments) with a 100-ms exposure time. For the image analysis, the regions of interest (ROIs, 3 \times 3 pixels) were first defined at the center (signal) and the neighboring areas (background) of each chamber; the mean intensity of each ROI was then calculated. We used the difference between the signal and the background intensity to obtain the fluorescence intensity of the reporter molecules in each chamber. The image analysis was performed using MATLAB software (MathWorks).

ASSOCIATED CONTENT

Supporting Information

Supporting equations and figures. This material is available free of charge via the Internet at <http://pubs.acs.org>.

AUTHOR INFORMATION

Corresponding Author

*Tel.: 81-6-6879-4171. Fax: 81-6-6879-7433. E-mail: Yomo@ist.osaka-u.ac.jp.

Author Contributions

T.O., T.M., and T.Y. conceived the project; T.O. performed the experiments and analyzed the data; T.O., T.M., and H.S. wrote the manuscript.

Notes

The authors declare no competing financial interest.

ACKNOWLEDGMENTS

We would like to thank Dr. Yasuaki Kazuta, Ms. Ryoko Otsuki, and Ms. Tomomi Sakamoto for producing the PURE system. This research was supported in part by JSPS KAKENHI Grant No. 24770153.

ABBREVIATIONS

GUS, β -glucuronidase; GAL, β -galactosidase

REFERENCES

- (1) Nagai, H., Murakami, Y., Morita, Y., Yokoyama, K., and Tamiya, E. (2001) Development of a microchamber array for picoliter PCR. *Anal. Chem.* 73, 1043–1047.
- (2) Rondelez, Y., Tresset, G., Nakashima, T., Kato-Yamada, Y., Fujita, H., Takeuchi, S., and Noji, H. (2005) Highly coupled ATP synthesis by F1-ATPase single molecules. *Nature* 433, 773–777.
- (3) Craighead, H. (2006) Future lab-on-a-chip technologies for interrogating individual molecules. *Nature* 442, 387–393.
- (4) Song, H., and Ismagilov, R. F. (2003) Millisecond kinetics on a microfluidic chip using nanoliters of reagents. *J. Am. Chem. Soc.* 125, 14613–14619.
- (5) Kinpara, T., Mizuno, R., Murakami, Y., Kobayashi, M., Yamaura, S., Hasan, Q., Morita, Y., Nakano, H., Yamane, T., and Tamiya, E. (2004) A picoliter chamber array for cell-free protein synthesis. *J. Biochem.* 136, 149–154.
- (6) Osaki, T., Yoshizawa, S., Kawano, R., Sasaki, H., and Takeuchi, S. (2011) Lipid-coated microdroplet array for *in vitro* protein synthesis. *Anal. Chem.* 83, 3186–3191.
- (7) Rissin, D. M., Gorris, H. H., and Walt, D. R. (2008) Distinct and long-lived activity states of single enzyme molecules. *J. Am. Chem. Soc.* 130, 5349–5353.
- (8) Rondelez, Y., Tresset, G., Tabata, K. V., Arata, H., Fujita, H., Takeuchi, S., and Noji, H. (2005) Microfabricated arrays of femtoliter chambers allow single molecule enzymology. *Nat. Biotechnol.* 23, 361–365.
- (9) Dittrich, P. S., Jahnz, M., and Schwill, P. (2005) A new embedded process for compartmentalized cell-free protein expression and on-line detection in microfluidic devices. *ChemBioChem* 6, 811–814.
- (10) Jung, S. Y., Liu, Y., and Collier, C. P. (2008) Fast mixing and reaction initiation control of single-enzyme kinetics in confined volumes. *Langmuir* 24, 4439–4442.
- (11) Abate, A. R., Hung, T., Mary, P., Agresti, J. J., and Weitz, D. A. (2010) High-throughput injection with microfluidics using picoinjectors. *Proc. Natl. Acad. Sci. U.S.A.* 107, 19163–19166.
- (12) Fallah-Araghi, A., Baret, J. C., Ryckelynck, M., and Griffiths, A. D. (2012) A completely *in vitro* ultrahigh-throughput droplet-based microfluidic screening system for protein engineering and directed evolution. *Lab Chip* 12, 882–891.
- (13) Cai, L., Friedman, N., and Xie, X. S. (2006) Stochastic protein expression in individual cells at the single molecule level. *Nature* 440, 358–362.
- (14) Thorsen, T., Roberts, R. W., Arnold, F. H., and Quake, S. R. (2001) Dynamic pattern formation in a vesicle-generating microfluidic device. *Phys. Rev. Lett.* 86, 4163–4166.
- (15) Xia, Y. N., and Whitesides, G. M. (1998) Soft lithography. *Angew Chem., Int. Ed.* 37, 551–575.
- (16) Fiordemondo, D., and Stano, P. (2007) Lecithin-based water-in-oil compartments as dividing bioreactors. *ChemBioChem* 8, 1965–1973.
- (17) Kato, A., Yanagisawa, M., Sato, Y. T., Fujiwara, K., and Yoshikawa, K. (2012) Cell-sized confinement in microspheres accelerates the reaction of gene expression. *Sci. Rep.* 2, 283.
- (18) Lizana, L., Konkoli, Z., Bauer, B., Jesorka, A., and Orwar, O. (2009) Controlling chemistry by geometry in nanoscale systems. *Annu. Rev. Phys. Chem.* 60, 449–468.
- (19) Jorgensen, P., and Tyers, M. (2004) How cells coordinate growth and division. *Curr. Biol.* 14, R1014–1027.
- (20) Saucedo, L. J., and Edgar, B. A. (2002) Why size matters: Altering cell size. *Curr. Opin. Genet. Dev.* 12, 565–571.
- (21) Rafelski, S. M., and Marshall, W. F. (2008) Building the cell: Design principles of cellular architecture. *Nat. Rev. Mol. Cell Biol.* 9, 593–602.
- (22) Kuthan, H. (2001) Self-organization and orderly processes by individual protein complexes in the bacterial cell. *Prog. Biophys. Mol. Biol.* 75, 1–17.
- (23) LeDuc, P., and Schwartz, R. (2007) Computational models of molecular self-organization in cellular environments. *Cell Biochem. Biophys.* 48, 16–31.
- (24) Matsuura, T., Hosoda, K., Kazuta, Y., Ichihashi, N., Suzuki, H., and Yomo, T. (2012) Effects of compartment size on the kinetics of intracompartamental multimeric protein synthesis. *ACS Synth. Biol.* 1, 431–437.
- (25) Okano, T., Matsuura, T., Kazuta, Y., Suzuki, H., and Yomo, T. (2012) Cell-free protein synthesis from a single copy of DNA in a glass microchamber. *Lab Chip* 12, 2704–2711.
- (26) Shimizu, Y., Inoue, A., Tomari, Y., Suzuki, T., Yokogawa, T., Nishikawa, K., and Ueda, T. (2001) Cell-free translation reconstituted with purified components. *Nat. Biotechnol.* 19, 751–755.
- (27) Kazuta, Y., Adachi, J., Matsuura, T., Ono, N., Mori, H., and Yomo, T. (2008) Comprehensive analysis of the effects of *Escherichia coli* ORFs on protein translation reaction. *Mol. Cell. Proteomics* 7, 1530–1540.
- (28) Matsuura, T., Kazuta, Y., Aita, T., Adachi, J., and Yomo, T. (2009) Quantifying epistatic interactions among the components constituting the protein translation system. *Mol. Syst. Biol.* 5, 297.
- (29) Matsuura, T., Hosoda, K., Ichihashi, N., Kazuta, Y., and Yomo, T. (2011) Kinetic analysis of β -galactosidase and β -glucuronidase tetramerization coupled with protein translation. *J. Biol. Chem.* 286, 22028–22034.
- (30) Jacobson, R. H., Zhang, X. J., DuBose, R. F., and Matthews, B. W. (1994) Three-dimensional structure of β -galactosidase from *E. coli*. *Nature* 369, 761–766.
- (31) Jain, S., Drendel, W. B., Chen, Z. W., Mathews, F. S., Sly, W. S., and Grubb, J. H. (1996) Structure of human β -glucuronidase reveals candidate lysosomal targeting and active-site motifs. *Nat. Struct. Biol.* 3, 375–381.
- (32) Urano, Y., Kamiya, M., Kanda, K., Ueno, T., Hirose, K., and Nagano, T. (2005) Evolution of fluorescein as a platform for finely tunable fluorescence probes. *J. Am. Chem. Soc.* 127, 4888–4894.
- (33) Schulz, H. N., and Jorgensen, B. B. (2001) Big bacteria. *Annu. Rev. Microbiol.* 55, 105–137.
- (34) Koch, A. L. (1996) What size should a bacterium be? A question of scale. *Annu. Rev. Microbiol.* 50, 317–348.
- (35) Soh, S., Banaszak, M., Kandere-Grzybowska, K., and Grzybowski, B. A. (2013) Why cells are microscopic: A transport-time perspective. *J. Phys. Chem. Lett.* 4, 861–865.
- (36) Lazzzerini-Ospri, L., Stano, P., Luisi, P., and Marangoni, R. (2012) Characterization of the emergent properties of a synthetic quasi-cellular system. *BMC Bioinformatics* 13 (Suppl 4), S9.
- (37) Goodsell, D. S., and Olson, A. J. (2000) Structural symmetry and protein function. *Annu. Rev. Biophys. Biomol. Struct.* 29, 105–153.
- (38) Forster, A. C., and Church, G. M. (2006) Towards synthesis of a minimal cell. *Mol. Syst. Biol.* 2, 45.
- (39) Simpson, M. L. (2006) Cell-free synthetic biology: A bottom-up approach to discovery by design. *Mol. Syst. Biol.* 2, 69.
- (40) Mann, S. (2012) Systems of creation: The emergence of life from nonliving matter. *Acc. Chem. Res.* 45, 2131–2141.
- (41) Luisi, P. L., Ferri, F., and Stano, P. (2006) Approaches to semi-synthetic minimal cells: A review. *Naturwissenschaften* 93, 1–13.
- (42) Stano, P., and Luisi, P. L. (2010) Achievements and open questions in the self-reproduction of vesicles and synthetic minimal cells. *Chem. Commun. (Camb.)* 46, 3639–3653.
- (43) Hosoda, K., Sunami, T., Kazuta, Y., Matsuura, T., Suzuki, H., and Yomo, T. (2008) Quantitative study of the structure of

multilamellar giant liposomes as a container of protein synthesis reaction. *Langmuir* 24, 13540–13548.

(44) Wu, H., Huang, B., and Zare, R. N. (2005) Construction of microfluidic chips using polydimethylsiloxane for adhesive bonding. *Lab Chip* 5, 1393–1398.